Shaping of ultrashort optical pulses by using an integrated acousto-optic tunable filter

M. E. Fermann,* V. da Silva, D. A. Smith, Y. Silberberg, and A. M. Weiner†

Bellcore, 331 Newman Springs Road, Red Bank, New Jersey 07701-7040

Received April 13, 1993

Reshaping of ultrashort optical pulses at 1.53 μm by using an integrated acousto-optic tunable filter is reported. Control of the optical pulse shape is accomplished by adjusting the different radio-frequency electrical signals driving the acousto-optic filter. This is to our knowledge the first demonstration of ultrashort pulse shaping using an integrated-optic device and establishes a new application area for integrated wavelength-division-multiplexed devices, namely, for manipulation of coherent, ultrafast time-domain signals.

A number of integrated-optic devices are being developed to filter, process, and route multiple-wavelength optical signals for wavelength-division-multiplexed (WDM) photonic networks. These include acousto-optic tunable filters,[1] spectrometers on a chip,[2] and multiplexers/demultiplexers based on arrayed waveguide gratings.[3,4] To date these devices have been used in situations in which individual optical wavelengths are independent and lack mutual phase coherence. However, these same devices can potentially be used to filter and reshape femtosecond optical pulses composed of a broad, mutually phase-locked band of wavelengths. In this Letter we report what is to our knowledge the first demonstration of femtosecond pulse shaping by using an integrated-optic WDM device. Previously, sophisticated pulse-shaping operations were performed by spatial filtering within a bulk-optics grating and lens apparatus,[5,6] and these shaped pulses were applied to studies of ultrafast fiber optics[7] and femtosecond spectroscopy.[8] The prospect of integrated pulse-shaping devices will facilitate the use of specially coded ultrafast optical waveforms in communications and other applications.

We performed our initial pulse-shaping experiments using an acousto-optic tunable filter (AOTF). Acousto-optic filters have broad applicability to WDM fiber communications because of their wide tuning range, narrow filter width, rapid switching time under electronic control, and capability for independent multiple optical wavelength operation. In integrated filters the optical input is coupled into a waveguide along one axis of a birefringent medium (typically $LiNbO_3$), and rf surface acoustic waves are used to transform the optical polarization state. Phase-matched polarization conversion occurs when the acoustic wavelength matches the polarization beat length, which varies with optical frequency. This results in a narrow-band polarization converter centered at an optical frequency controlled by the rf drive frequency. By placing this device between polarizers, we obtain a narrow-band optical filter. Multiple optical wavelengths can be filtered simultaneously and independently by application of multiple rf drive frequencies. In WDM networks this capability is particularly useful for applications such as gain equalization for erbium fiber amplifier chains[9] or implementation of add–drop multiplexers,[10] since individual wavelengths can be attenuated or rerouted independently. This same multiple-wavelength filtering capability is also particularly useful for femtosecond pulse shaping. The concept is to pass an ultrashort pulse, containing many optical frequencies, through the AOTF and to apply multiple electrical drive frequencies to filter the different optical frequencies independently. The difference between the pulse-shaping operation and the standard multiwavelength operation is that for pulse shaping both the amplitude and the phase response of the AOTF determine the form of the reshaped pulse.

For our pulse-shaping experiments a single-stage AOTF was used in a notch filter configuration, i.e., with a polarized input optical signal and with the output polarizer aligned to pass the input polarization. This avoids the frequency shifts associated with TE-to-TM-mode conversion that occur in the normal bandpass filter operating mode; such frequency shifts would lead to time-varying phase shifts and pulse shapes that vary with time. Furthermore, to avoid time-dependent coherent grating cross talk, the grating resonance wavelengths have to be well separated, i.e., by approximately twice the grating bandwidth. When N acoustic gratings are present in the AOTF, the overall transfer function of the device operating in notch filter mode may be written as

$$T(\omega) = 1 - \sum A_j(\kappa_j, \omega - \alpha\Omega_j), \qquad (1)$$

where $A_j = 1 - T_j(\kappa_j, \omega - \alpha\Omega_j)$ is the light coupled over to the other polarization state by each individual grating. A_j has both amplitude and phase components and depends on the mode-coupling parameter κ_j, the optical frequency ω, and the acoustic drive frequency Ω_j. α is a factor that scales the acoustic drive frequency to the optical resonance frequency. In our filter we have $\alpha \approx 1.1 \times 10^6$. It is then easy to show that the output waveform for a δ-function input pulse (i.e., a pulse with a spectral bandwidth much

0146-9592/93/181505-03$6.00/0

larger than the grating bandwidth) is given by

$$E_{\text{out}}(t) = \delta(t) - F\{A_0(\omega)\}\sum \exp(i\alpha\Omega_j t). \qquad (2)$$

Here $A_0(\omega) = 1 - T_0(\omega)$ is the line shape of a single grating, $F\{A_0(\omega)\}$ is the Fourier transform of $A_0(\omega)$, and, for simplicity, we have assumed that all gratings have the same coupling strength κ. We see that different pulse shapes may be generated by selecting the frequencies Ω_j. The maximum duration of the shaped pulse in the time domain is proportional to the inverse of the filter bandwidth in the frequency domain. This means that the output waveform is generated in a time window corresponding to the group-velocity walk-off between the two polarization axes of the AOTF. For a 2.3-cm-long filter and a typical refractive-index difference between the two polarization axes of 0.07, we thus obtain a time window of 5.4 ps, and hence the AOTF is particularly suitable for the processing of ultrafast waveforms on time scales of femtoseconds up to several picoseconds.

The experimental setup is shown in Fig. 1. An additive-pulse mode-locked color-center laser generates pulses 100 fs in duration at a center wavelength of 1.53 μm and a repetition rate of 82 MHz. The output of the laser is split into two beams. One beam is amplified with an erbium-doped fiber amplifier, which narrows the spectrum to ~10 nm and broadens the pulse duration to ~500 fs. The amplified beam is then coupled into a fiber-pigtailed AOTF for shaping. The second beam serves as a source of 100-fs reference pulses used to measure the temporal intensity profile of the shaped pulses through intensity cross correlation.

Our initial demonstration of pulse shaping was performed by driving a single-stage AOTF with two separate electrical (hence acoustic) frequencies near a center frequency of 175 MHz. The device had a 23-mm interaction length and is described in detail in Ref. 11. The two electrical drives lead to two notches in the transmitted spectrum at the optical frequencies where resonant polarization conversion occurs. Each electrical drive had a power of ~11 dBm, corresponding to maximum extinction of the filtered optical frequency. A series of experiments with notch separations ranging from 3 to 10 nm were performed. Figure 2 shows a spectrum measured after the AOTF for a notch separation $\delta\lambda$ of 4 nm. The incomplete extinction at the filtered frequencies occurs most likely as a result of the polarization sensitivity of our acousto-optic filter. Measurements of the corresponding time-domain waveforms are shown in Fig. 3 for input pulses launched along the slow or fast axis of the AOTF. As expected from Eq. (2), the output waveforms consist of two portions. The first is a strong pulse at $t = 0$, which arrives at the same time as the pulse transmitted through the AOTF when the drive signals are turned off [Fig. 3(a)]. The second weaker portion corresponds to the pulse reshaping by the AOTF [the second term in Eq. (2)]. In these experiments the reshaped portion corresponds to a beat pattern in the time domain, with the beat period $\delta t = \lambda^2/c\delta\lambda$ corresponding to the inverse of the notch separation in the frequency domain. The measured beat period in Fig. 3, as well as the periods observed for experiments performed with other notch separations, are in good agreement with this simple formula. Note also that the reshaped portion of the pulse is less intense than the pulse transmitted at $t = 0$. This arises because the energy contained in the two notches responsible for pulse reshaping is much less than the energy remaining in the unfiltered portion of the spectrum, which is responsible for the peak at $t = 0$.

The fact that the beat pattern occurs only for $t < 0$ in Fig. 3(b) and only for $t > 0$ in Fig. 3(c) deserves further comment. The transit time τ for a light pulse to pass through the AOTF is bounded by $n_f L/c < \tau < n_s L/c$, where n_f and n_s are the refractive indexes for light polarized along the fast and slow axes, respectively, L is the length of the device, and c is the speed of light. For a pulse launched along the slow axis, reshaping in the time domain arises when a portion of the light is induced to travel along the fast axis through parts of the device. This light traveling along the fast axis through parts of the device emerges in a time less than $n_s L/c$, hence before the main pulse at $t = 0$. Thus, for input pulses polarized along the slow axis, reshaping can occur only for $t < 0$. Similarly, for light launched along the fast axis, the reshaped pulse can be generated only for $t > 0$.

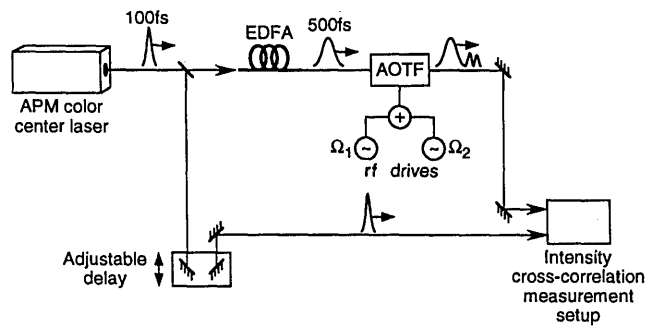

Fig. 1. Experimental setup. Pulses from an additive-pulse mode-locked (APM) color-center laser at 1.53 μm are amplified and broadened in an erbium-doped fiber amplifier (EDFA) and then shaped by a fiber-pigtailed AOTF driven by two electrical signals at frequencies Ω_1 and Ω_2. The shaped pulse is measured by intensity cross correlation with 100-fs pulses directly from the APM laser.

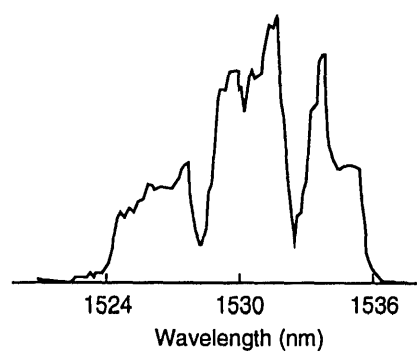

Fig. 2. Optical power spectrum measured after transmission through the AOTF, showing two notches separated by 4 nm.

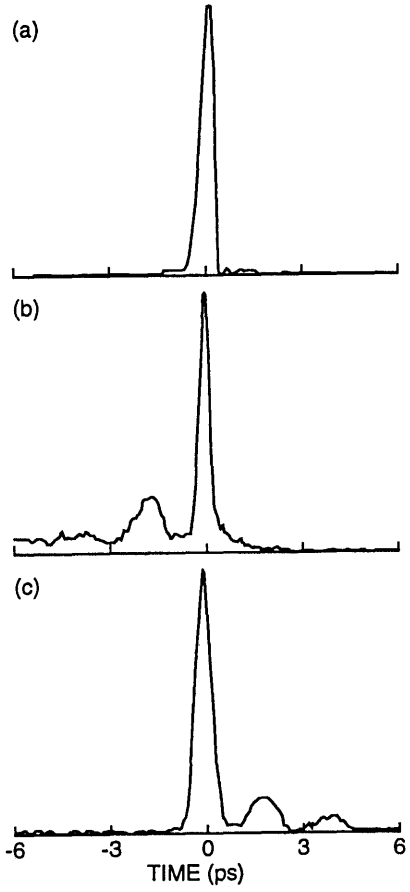

Fig. 3. Intensity cross-correlation measurements of the waveforms emerging from the AOTF. (a) Transmitted pulse measured with the drives to the filter turned off. (b), (c) Reshaped pulses corresponding to two notches separated by 4 nm; in (b) the input pulse is launched along the slow axis of the birefringent medium, whereas in (c) the input pulse is launched along the fast axis.

With reference to Eq. (2), this means that $F\{A_0(\omega)\}$ is zero for $t > 0$ ($t < 0$) for input pulses polarized along the slow (fast) axis. This causality condition implies that the phase and amplitude of the filter response $A(\omega)$ are linked by a Kramers–Kronig relation. This causality condition affecting the AOTF is similar to the causality condition governing the dielectric response functions of materials, in which the phase and amplitude of the spectral line shape are also linked by the Kramers–Kronig relation.

More complex pulse-shaping operations can be implemented by using more than two acoustic gratings. Typical passbands for a single-stage AOTF are of the order of a nanometer; narrower linewidths can be obtained by using cascaded filters or longer devices. Since 100-fs pulses at 1.5 μm can have bandwidths approaching 40 nm, even AOTF's with passbands as large as 1 nm can potentially generate shaped pulses or code sequences with rather considerable complexity.

In conclusion, we have demonstrated a new application area for integrated WDM devices, namely, for manipulating coherent ultrafast time-domain signals. In the future we plan to go beyond our initial experiments by using a more sophisticated, two-stage AOTF design.[1] The two-stage AOTF will allow pulse-shaping operation in the preferred bandpass configuration without imposing undesirable optical frequency shifts and will make possible independent spectral phase and amplitude control for complete pulse-shaping control. This would bring together the powerful capabilities previously achieved by using bulk-optics pulse shapers with the additional advantages of a completely integrated device and electronic programmability on the microsecond time scale.

We gratefully thank John Johnson for fabrication of the AOTF used in these experiments. M. E. Fermann acknowledges financial support from the Alexander von Humboldt Stiftung.

*Present address, IMRA America, Inc., 1044 Woodbridge Avenue, Ann Arbor, Michigan 48105.

†Present address, School of Electrical Engineering, Purdue University, West Lafayette, Indiana 47907-1285.

References

1. D. A. Smith, J. E. Baran, J. J. Johnson, and K. W. Cheung, IEEE J. Select. Areas Commun. **8,** 1151 (1990).
2. J. B. D. Soole, A. Scherer, H. P. LeBlanc, N. C. Andreadakis, R. Bhat, and M. A. Koza, Electron. Lett. **27,** 132 (1991).
3. C. Dragone, IEEE Photon. Technol. Lett. **3,** 812 (1992).
4. H. Takahashi, I. Nishi, and Y. Hibino, Electron. Lett. **28,** 380 (1992).
5. A. M. Weiner, J. P. Heritage, and E. M. Kirschner, J. Opt. Soc. Am. B **5,** 1563 (1988).
6. A. M. Weiner, D. E. Leaird, J. S. Patel, and J. R. Wullert, IEEE J. Quantum Electron. **28,** 908 (1992).
7. A. M. Weiner, J. A. Salehi, J. P. Heritage, and M. Stern, in *Photonic Switching,* Vol. 3 of OSA Proceedings Series, J. E. Midwinter and H. S. Hinton, eds. (Optical Society of America, Washington, D.C., 1989), pp. 263–269.
8. A. M. Weiner, D. E. Leaird, G. P. Wiederrecht, and K. A. Nelson, Science **247,** 1317 (1990).
9. S. F. Su, R. Olshansky, G. Joyce, D. A. Smith, and J. E. Baran, IEEE Photon. Technol. Lett. **4,** 269 (1992).
10. W. I. Way, D. A. Smith, J. J. Johnson, and H. Izadpanah, IEEE Photon. Technol. Lett. **4,** 402 (1992).
11. D. A. Smith and J. J. Johnson, IEEE Photon. Technol. Lett. **3,** 923 (1991).